Electronic Supplementary Information

High-Performance Hybrid White Organic Light-Emitting Diodes with Simple Emitting Structures and Low Efficiency Roll-off Based on Blue Thermally Activated Delayed Fluorescence Emitter with Bipolar Transport Characteristic

Chenyang Zhao,[ab] *Tianmu Zhang,*[a] *Jiangshan Chen,*[c] *Donghang Yan*[*a] *and Dongge Ma*[*ac]

[a]State Key Laboratory of Polymer Physics and Chemistry, Changchun Institute of Applied Chemistry, Chinese Academy of Sciences, Changchun130022, P. R. China.

[b]University of Science and Technology of China, Hefei 230026, P. R.China.

[c]Institute of Polymer Optoelectronic Materials and Devices, State Key Laboratory of Luminescent Materials and Devices, South China University of Technology, Guangzhou 510640, P. R. China.

*Email: cyzhao@ciac.ac.cn

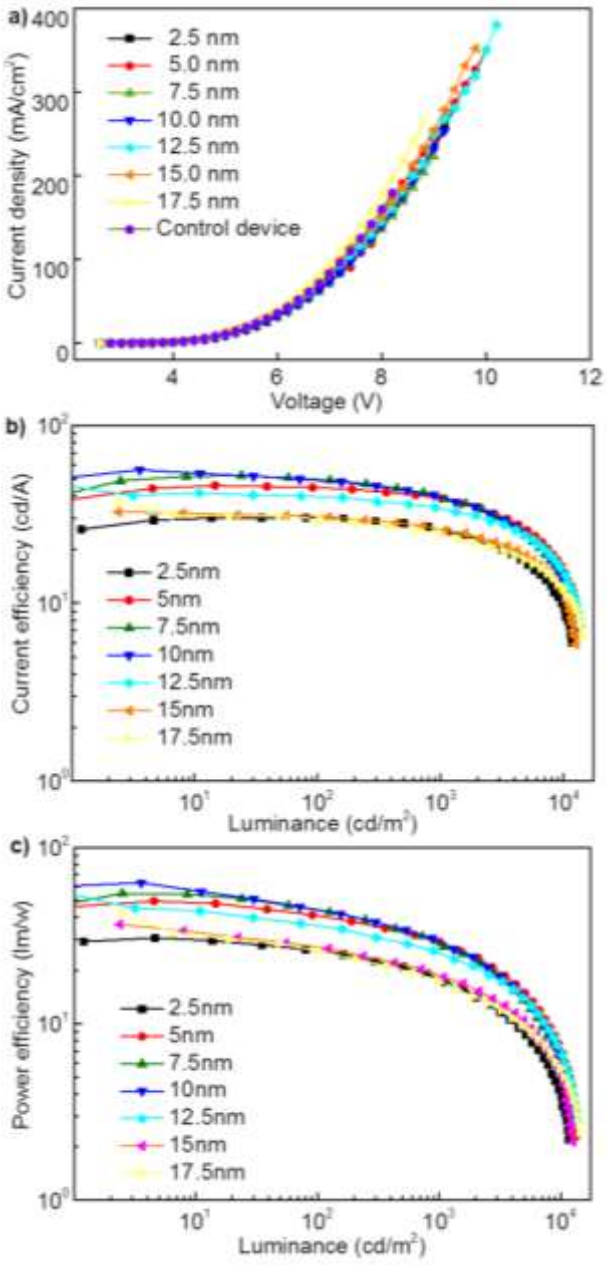

Figure S1. a) *J-V* characteristics of the blue devices with ultrathin phosphorescent orange layer of PO-01 (0.06 nm PO-01) inserted into the different position of the EML.The position of the interface between mCP and DMAC-DPS is recorded as 0 nm. *x* ranges from 2.5 nm to 17.5 nm away from the interface to the EML of DMAC-DPS with the interval thickness of 2.5 nm.b) Current efficiency versus luminance characteristics. c) Power efficiency versus luminance characteristics.

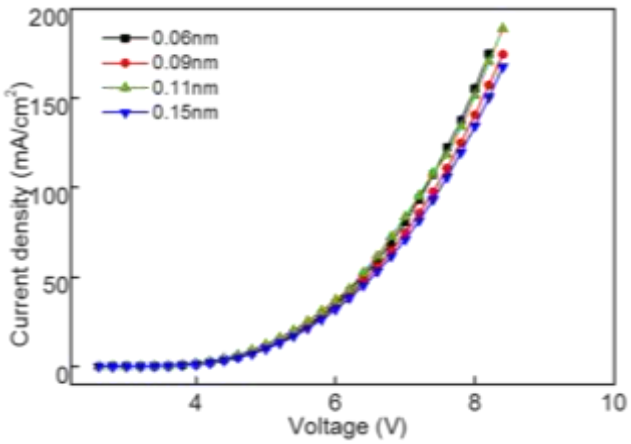

Figure S2. *J-V* characteristics of devices by increasing the thickness of the ultrathin phosphorescent orange layer of PO-01.

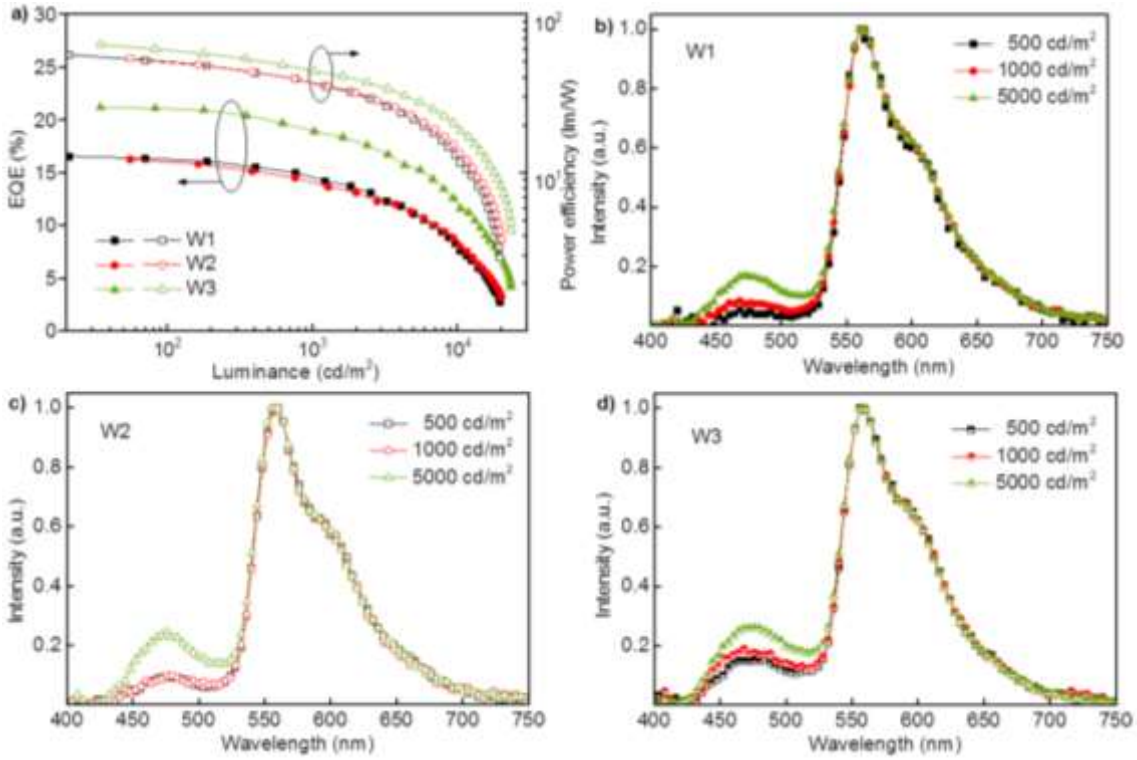

Figure S3. a) EQE and power efficiency characteristics versus luminanceof Device W1, W2, W3. b) EL spectra of Device W1 at the different luminance of 500 cd m^{-2}, 1000 cd m^{-2}, and 5000 cd m^{-2}. c) EL spectra of Device W2 at the different luminance of 500 cd m^{-2}, 1000 cd m^{-2}, and 5000 cd m^{-2}. d) EL spectra of Device W3 at the different luminance of 500 cd m^{-2}, 1000 cd m^{-2}, and 5000 cd m^{-2}.

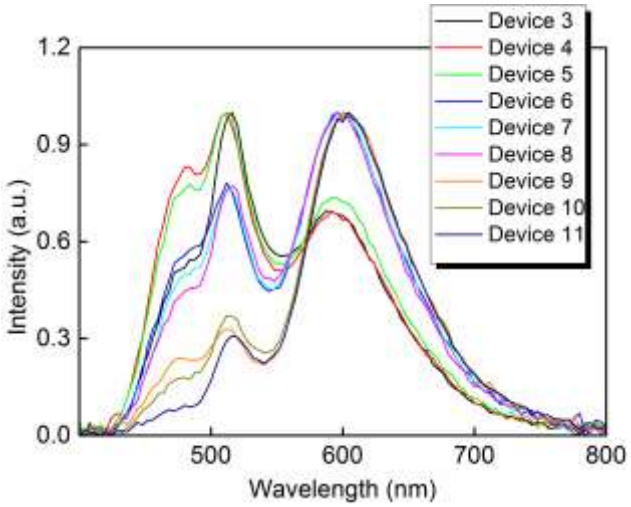

Figure S4. Spectra of hybrid WOLEDs with different thicknesses of $Ir(MDQ)_2(acac)$ and $Ir(ppy)_2(acac)$ at the luminance of 1000 cd m^{-2}. *X-Y*represents X nm $Ir(MDQ)_2(acac)$ and Y nm $Ir(ppy)_2(acac)$. The thicknesses of $Ir(MDQ)_2(acac)$ and $Ir(ppy)_2(acac)$ in Device 3-Device 11 are 0.02-0.06, 0.02-0.09, 0.02-0.12, 0.03-0.06, 0.03-0.09, 0.03-0.12, 0.05-0.06, 0.05-0.09, and 0.05-0.12, respectively.

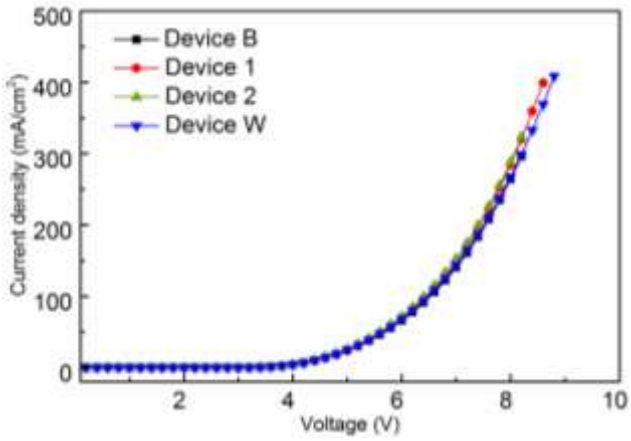

Figure S5. *J-V-L* characteristics of Device B, 1, 2, and W. The EMLs of them are DMAC-DPS (20 nm) (Device B), DMAC-DPS (10 nm)/$Ir(ppy)_2(acac)$ (0.09 nm)/DMAC-DPS (10 nm) (Device 1), DMAC-DPS (7.5 nm)/$Ir(MDQ)_2(acac)$ (0.03 nm)/DMAC-DPS (5 nm)/$Ir(ppy)_2(acac)$ (0.03 nm)/DMAC-DPS (7.5 nm) (Device 2), DMAC-DPS (7.5 nm)/$Ir(MDQ)_2(acac)$ (0.03 nm)/DMAC-DPS (2.5 nm)/$Ir(ppy)_2(acac)$ (0.09 nm)/DMAC-DPS (2.5 nm)/$Ir(MDQ)_2(acac)$ (0.03 nm)/DMAC-DPS (7.5 nm) (Device W), respectively.

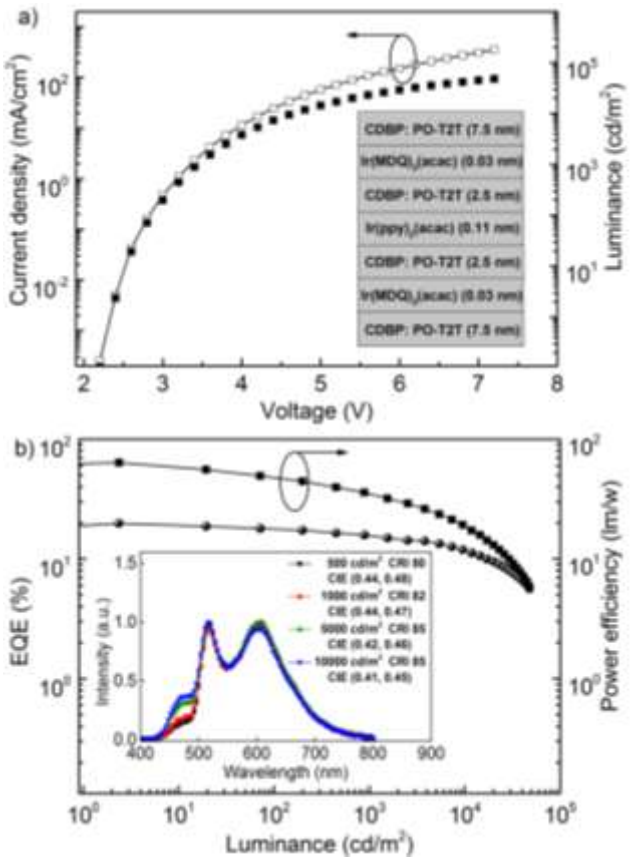

Figure S6. a) Current density-luminance-voltage characteristics of Device E. The inset shows the structure of the EML in Device E. b) EQE and power efficiency characteristics versus luminance of Device E. The inset shows the normalized EL spectra and corresponding CRIs and CIEs at different luminance of Device E. The complete configuration of Device E is ITO(180 nm)/MoO_3 (8 nm)/TCTA: MoO_3 (15%, 50 nm)/TCTA (10 nm)/CDBP (10 nm)/CDBP: PO-T2T(1:1, 7.5 nm)/$Ir(MDQ)_2(acac)$ (0.03 nm)/CDBP: PO-T2T (1:1, 2.5 nm)/$Ir(ppy)_2(acac)$ (0.11 nm)/CDBP: PO-T2T (1:1, 2.5 nm)/$Ir(MDQ)_2(acac)$ (0.03 nm)/CDBP: PO-T2T (1:1, 7.5 nm)/PO-T2T (10 nm)/PO-T2T: Li_2CO_3 (3%, 45 nm)/Li_2CO_3 (1 nm)/Al.

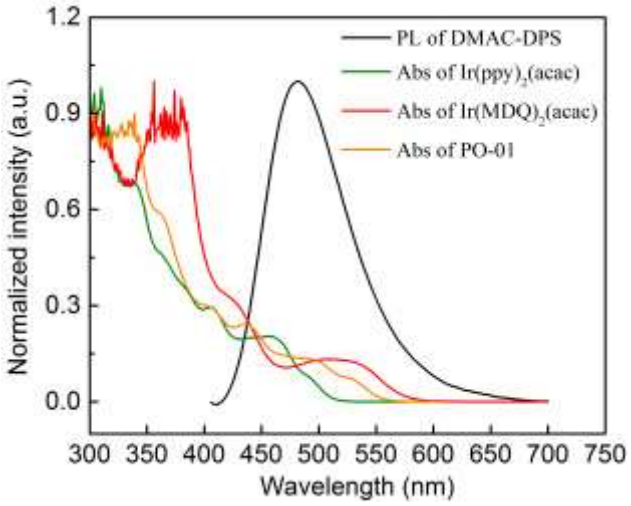

Figure S7. PL spectrum of DMAC-DPS and absorption spectra of phosphorescent emitters.

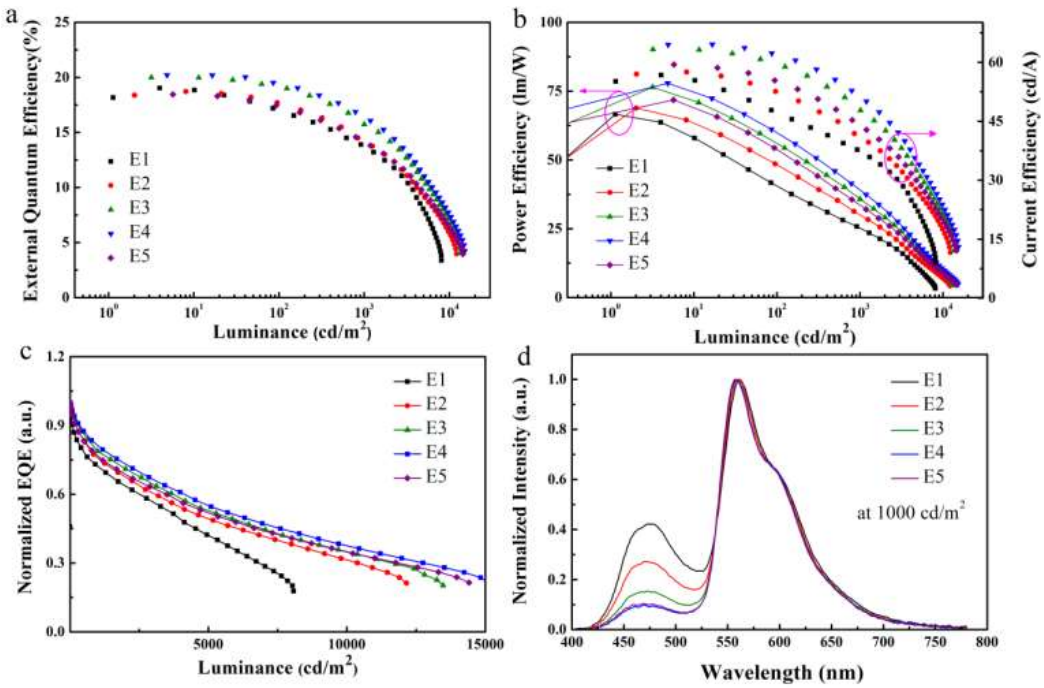

Figure S8. a) EQE characteristics versus luminance of Device E1-E5. b) Power efficiency and current effuciency characteristics versus luminanceof Device E1-E5. c) Normalized EQE characteristics versus luminanceof Device E1-E5. d) EL spectra of Device E1-E5 at the luminance of 1000 cd m^{-2}. The EML sructures of Device E1-E5 are DMAC-DPS (10nm)/PO-01 (0.15nm)/DMAC-DPS (10nm) (E1), DMAC-DPS (8.75nm)/PO-01 (0.075nm)/DMAC-DPS (2.5nm)/PO-01 (0.075nm)/DMAC-DPS (8.75nm) (E2), DMAC-DPS (7.5nm)/PO-01 (0.05nm)/DMAC-DPS (2.5nm)/PO-01 (0.05nm)/DMAC-DPS (2.5nm)/PO-01 (0.05nm)/DMAC-DPS (7.5nm) (E3), DMAC-DPS (3.75nm)/PO-01 (0.038nm)/DMAC-DPS (2.5nm)/PO-01 (0.038nm)/DMAC-DPS (2.5nm)/PO-01 (0.038nm)/DMAC-DPS (2.5nm)/PO-01 (0.038nm)/DMAC-DPS (3.75nm) (E4), DMAC-DPS (2.5nm)/PO-01 (0.03nm)/DMAC-DPS (2.5nm)/PO-01 (0.03nm)/DMAC-DPS (2.5nm)/PO-01 (0.03nm)/DMAC-DPS (2.5nm)/PO-01 (0.03nm)/DMAC-DPS (2.5nm)/PO-01 (0.03nm)/DMAC-DPS (2.5nm) (E5).

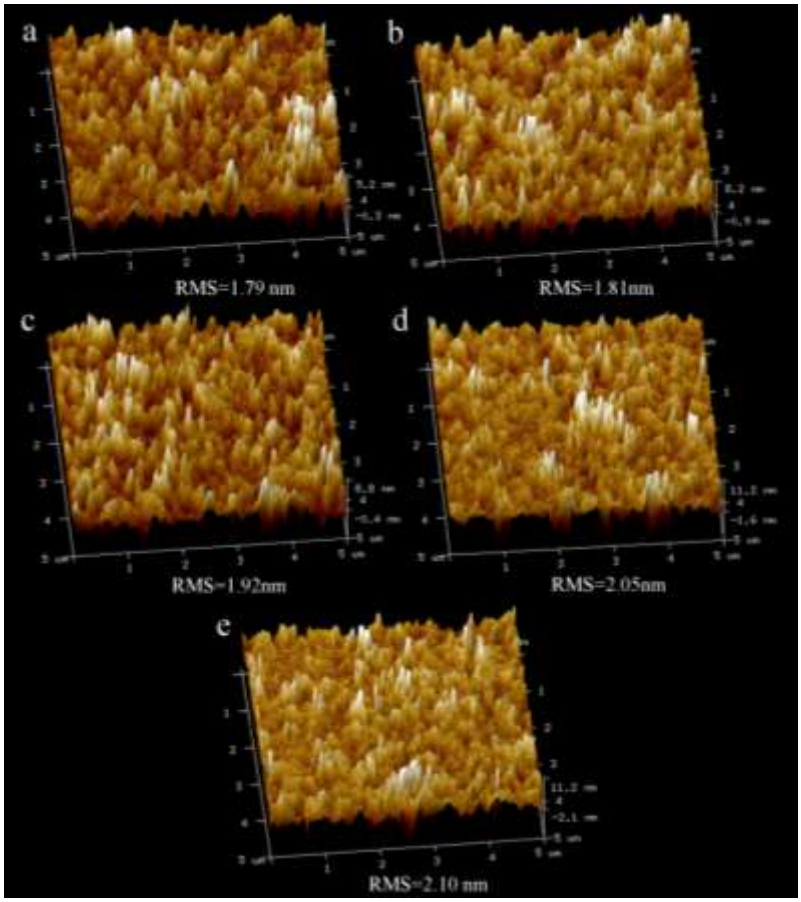

Figure S9. The high resolution resolution atomic force microscope images of films ((DMAC-DPS (20 nm)/PO-01 (0 nm, 0.03 nm, 0.09 nm, 0.15 nm, 0.25 nm)).

Table S1. Key performances of hybrid WOLEDs with different thicknesses of Ir(MDQ)$_2$(acac) and I (ppy)$_2$(acac).

	X-*Y*	Max CE/PE [cd A^{-1}/lm W^{-1}]	Performance at the luminance of 1000 cd m^{-2}			
			CE/PE [cd A^{-1}/lm W^{-1}]	CRI (*x*, *y*)	CIE	CCT
Device 3	0.02-0.06	42.8/44.2	37.6/28.8	(0.36, 0.44)	77	4806
Device 4	0.02-0.09	42.4/47.5	32.7/25.1	(0.33, 0.40)	81	5448
Device 5	0.02-0.12	40.4/41.4	34.2/26.1	(0.35, 0.40)	82	5093
Device 6	0.03-0.06	39.1/36.6	36.1/27.5	(0.41, 0.41)	83	3494
Device 7[a]	0.03-0.09	41.6/42.4	39.2/30.9	(0.42, 0.42)	83	3414
Device 8	0.03-0.12	40.6/40.2	38.5/30.2	(0.42, 0.43)	83	3436
Device 9	0.05-0.06	25.8/25.8	23.9/18.1	(0.49, 0.40)	74	2235
Device 10	0.05-0.09	27.3/27.1	25.6/19.1	(0.50, 0.42)	76	2287
Device 11	0.05-0.12	26.8/26.7	25.2/19.1	(0.52, 0.43)	74	2102

[a]Device 7 is hybrid WOLED of Device W.